Sensors and Actuators B 193 (2014) 857–863

Contents lists available at ScienceDirect

Sensors and Actuators B: Chemical

journal homepage: www.elsevier.com/locate/snb

FITC functionalized magnetic core–shell Fe_3O_4/Ag hybrid nanoparticle for selective determination of molecular biothiols

Ling Chen[a,d], Jinhua Li[a], Shasha Wang[a,d], Wenhui Lu[a], Aiguo Wu[b], Jaebum Choo[c], Lingxin Chen[a,*]

[a] Key Laboratory of Coastal Environmental Processes and Ecological Remediation, Yantai Institute of Coastal Zone Research, Chinese Academy of Sciences, Yantai 264003, China
[b] Key Laboratory of Magnetic Materials and Devices, and Division of Functional Materials and Nanodevices, Ningbo Institute of Materials Technology and Engineering, Chinese Academy of Sciences, Ningbo 315201, China
[c] Department of Bionano Technology, Hanyang University, Ansan 426-791, South Korea
[d] University of Chinese Academy of Sciences, Beijing 100049, China

ARTICLE INFO

Article history:
Received 3 October 2013
Received in revised form 6 December 2013
Accepted 12 December 2013
Available online 21 December 2013

Keywords:
Molecular biothiols
Chromogenic detection
Silver-coated magnetic nanoparticles
Fluorescein isothiocyanate
Living cells

ABSTRACT

A sensing strategy for chromogenic detection of molecular biothiols has been proposed based on fluorescein isothiocyanate (FITC) functionalized magnetic core–shell Fe_3O_4/Ag hybrid nanoparticles. Ag coated magnetic Fe_3O_4 nanoparticles were initially synthetized. FITC was subsequently conjugated on the surface of core–shell nanoparticles by Ag–SCN linkage and then the fluorescence of FITC was quenched. Upon addition of molecular biothiols, since the Ag—S bond is stronger than Ag–SCN, a place-displacement between thiols and FITC would occur and thereby the fluorescence of FITC would recover. Thus, a fluorescence "off-on" probe was attained by virtue of biothiols, so after magnetic separation, the fluorescence signal change of FITC in clear solution could be employed for quantitative determination of typical molecular biothiols such as glutathione (GSH) and cysteine (Cys). High sensitivity was obtained with the detection limits of 10 nM and 20 nM for GSH and Cys, respectively. As well as, the assay strategy presented excellent selectivity toward molecular biothiols against other amino acids. Furthermore, confocal imaging was achieved in living cells, indicating that this fluorescent probe is potentially applicable for imaging molecular thiols in biological systems.

1. Introduction

Molecular biothiols are known to play pivotal roles in a variety of important biological processes, such as reversible redox reactions and cellular functions including detoxification and metabolism [1,2]. The concentrations of certain thiols have been associated with a number of diseases. Specifically, glutathione (GSH), composed of glutamic acid, cysteine and glycine, is a ubiquitous tripeptide and the principal nonprotein thiol. It has vital roles in maintenance of intracellular redox activity, intracellular signal transduction, and gene regulation [3]. Abnormal changes in the concentrations of GSH in plasma and erythrocytes are very possibly linked to HIV syndrome [4,5], Alzheimer's disease [6], or Werner syndrome [7]. Cysteine (Cys) is a nonessential amino acid, the lack of which can result in many syndromes, such as slow growth in children, liver damage, skin lesions, and loss of muscle [8,9].

Accordingly, the identification and detection of molecular biothiols in biological systems is required and very important. In recent years, a great amount of interesting studies have focused on the determination and sensing of biothiols. Various analytical methods including high-performance liquid chromatography [10,11], capillary electrophoresis [12,13], mass spectrometry [14], chemiluminescence [15,16], electrochemistry assay [17,18], fluorimetry [19–21], and nanoparticles-based colorimetric sensing strategy [22–27] for biothiols have been developed. Among these methods, fluorescent probes and gold-nanoparticle-based colorimetric sensing gradually stand out in the rapid, sensitive, and selective determination of biothiols. Fluorescent probes have attracted great attention on account of their abilities to make thiols "visible" in living cells and to provide greater sensitivity. Our team has developed a series of fluorescent probes that can be used for rapid detection of thiols under physiological conditions, with emission in the near infrared (NIR) region [28,29]. Yet, in most of the reported fluorescent methods, organic solvents are required to be introduced into the system to increase the solubility of fluorescent dyes [19–21]. As a type of recently developed biothiol sensor, gold-nanoparticle-based colorimetric sensing in general involves the aggregation,

* Corresponding author. Tel.: +86 535 2109130; fax: +86 535 2109130.
E-mail address: lxchen@yic.ac.cn (L. Chen).

0925-4005/$ – see front matter © 2013 Elsevier B.V. All rights reserved.
http://dx.doi.org/10.1016/j.snb.2013.12.053

coupling, or assembly of gold nanospheres [22,23] and nanorods [24,25]. The dynamic process of nanoparticles assembly is strongly sensitive to the surrounding environment which should be carefully controlled in order to obtain reproducible assemblies.

Herein, water soluble magnetic core–shell Fe_3O_4/Ag hybrid nanoparticles were prepared and the silver shell was employed as a carrier and fluorescence quencher of fluorescein isothiocyanate (FITC) by Ag–SCN linkage. The biothiols were sensed by the fluorescence recovery of FITC based on a place-exchange between thiols and FITC which relied on the fact that Ag—S bond is stronger than Ag–SCN. For this reason, the sensitivity and selectivity of this sensing system were investigated using GSH and Cys as the models of biothiols.

2. Experimental

2.1. Chemicals

Fluorescein isothiocyanate (FITC), glutathione (GSH), cysteine (Cys), alanine (Ala), lysine (Lys), tryptophan (Trp), glycine (Gly), polyethylene glycol, mercapto propyl trimethoxy silane (MPTS), and thiol-reactive n-ethyl-maleimide (NEM) were purchased from Aladdin (Shanghai, China). Other regents such as silver nitrate ($AgNO_3$), ferric chloride hexahydrate ($FeCl_3{\cdot}6H_2O$), sodium acetate (NaAc) were received from Sinopharm Chemical Reagent Co., Ltd, China (Shanghai, China). All of the reagents were of analytical grade and used without future purification.

2.2. Instrumentation

Solutions were prepared with deionized water (18.2 MΩ cm specific resistances) purified by a Cascada TM LS Ultrapure water system (Pall Corp., USA). UV–vis absorption spectra were measured on a Thermo Scientific NanoDrop 2000/2000C spectrophotometer (USA). Dynamic light scattering (DLS) measurements were performed on a Malvern Zetasizer Nano-ZS90 (ZEN3590, UK). The morphological evaluation was carried out by scanning electron micrography (SEM, JSM 5600 LV, operating at 20 kV). IR spectra were obtained on a Nicolet iS 10 FT-IR spectrometer (Thermo Fisher Scientific, USA). Fluorescence spectra were obtained on a FluoroMax-4 Spectrofluorometer with a xenon lamp and 1.0 cm quartz cells (Japan). Fluorescence imaging was performed by confocal fluorescence microscopy on an Olympus FluoView Fv1000 laser scanning microscope (USA). The pH measurements were carried out on a PHS-3C meter (Shanghai, China).

2.3. Synthesis of core–shell Fe_3O_4/Ag nanoparticles

Firstly, Fe_3O_4 nanoparticles were synthesized according to the reported method [30] with slight necessary modifications. Typically, $FeCl_3{\cdot}6H_2O$ (1.35 g, 5 mmol) was dissolved in ethylene glycol (40 mL) to form a clear solution, followed by the addition of NaAc (3.6 g) and polyethylene glycol (4.0 g). The mixture was stirred vigorously for 30 min and then sealed in a Teflon lined stainless-steel autoclave (50 mL capacity). The autoclave was heated to and maintained at 200 °C for 8 h, and allowed to cool to room temperature. The black products were washed several times with ethanol and dried at 60 °C for 6 h.

The silver shell was coated on the surface of Fe_3O_4 nanoparticles according to the reported protocol [31]. The specific synthetic route was shown in Fig. S1 in Supporting Information. Firstly, magnetite particles were treated with MPTS. Fe_3O_4 (0.129 g) and MPTS (0.8 mL) were mixed in 40 mL ethanol (C_2H_5OH), refluxing at 80 °C for 6 h. The products were washed several times with ethanol. An $Ag[(NH_3)_2]^+$ solution was obtained by mixing 50 mg $AgNO_3$ with 0.5 mL ammonia water in 50 mL of deionized water and sodium hydroxide was used to adjust the pH value of the solution to 13.0. Then, 45 mg Fe_3O_4 microspheres were stirred into the solution, and the mixture was stirred for 1 h. The mixture of 5 mL HCHO and 20 mL ethanol were dropped into the solution with stirring for 8 h. The products were separated by magnetic fields and then were washed with ethanol.

2.4. Modification of core–shell Fe_3O_4/Ag nanoparticles with FITC

A 50 mL FITC ethanol solution (1 mM) was mixed with 50 mL aqueous solution containing Fe_3O_4/Ag hybrid nanoparticles (1 mg/mL), and the mixture was kept at 37 °C for 3 h. The product was washed several times with deionized water to remove excess FITC by magnetic separation.

2.5. Determination of molecular biothiols

In a general procedure, under optimum conditions, 80 μL of FITC modified Fe_3O_4/AgNPs hybrid material aqueous solution (1 mg/mL) was added to the 1900 μL sodium acetate buffer solution (10 mM), followed by addition of 20 μL molecular biothiol solutions at different concentrations. Then, the mixture was incubated at 37 °C for 20 min. After that, the mixture was separated by magnetic fields and the above clear solution was measured for fluorescence spectra. For all measurements, emission slit width was 4 nm, excitation wavelength was 490 nm and the fluorescence intensity was acquired with emission at 514 nm.

In the experiments of selectivity assay, all samples were tested in a similar manner. The selectivity of the sensing approach toward molecular biothiols was investigated over other amino acids.

2.6. Cell culture and confocal imaging

Hela cell lines (human cervical carcinoma cells) were obtained from the cell bank of Shanghai Institute of Biochemistry and Cell Biology (Shanghai, China). Cells were cultured in DMEM Medium supplemented with 10% fetal bovine serum (FBS) at 37 °C in a humidified atmosphere containing 5% CO_2. Hela cells placed on coverslips were washed with phosphate buffered saline (PBS), followed by incubating with FITC modified Fe_3O_4/Ag nanoparticles. Fluorescence imaging of intracellular GSH in Hela cells was conducted by using a confocal fluorescence microscopy on an Olympus FluoView Fv1000 laser scanning microscope with ×20 and ×40 objective lenses. The excitation wavelength was 490 nm. Cell imaging was carried out after washing three times with PBS.

3. Results and discussion

3.1. Characterization of the Fe_3O_4/Ag hybrid nanoparticles

Characterization of the Fe_3O_4/Ag hybrid nanoparticles was shown in Fig. S2 in Supporting Information. As indicated in Fig. S2A, the UV–vis spectrum of the prepared particles showed a surface plasmon resonance peak at about 440 nm indicating the formation of silver shell coated on magnetic nanoparticles. The SEM image was obtained from dried nanoparticles which were directly adhered to the sample stage, instead of decentralized solution, thereby, the particles exhibited aggregated state. The size of prepared nanoparticles was estimated about 80–120 nm as shown in SEM image (Fig. S2B). Moreover, the size distribution of nanoparticles was obtained by DLS measurement. It tends to overestimate the diameters of nanoparticles measured by SEM images because DLS measured hydrodynamic diameters of silver coated hybrid nanoparticles. As indicated by Fig. S2C, the intensity contribution versus diameters of nanoparticles displayed a good size-distribution and a dominant distribution peak around 200 nm;

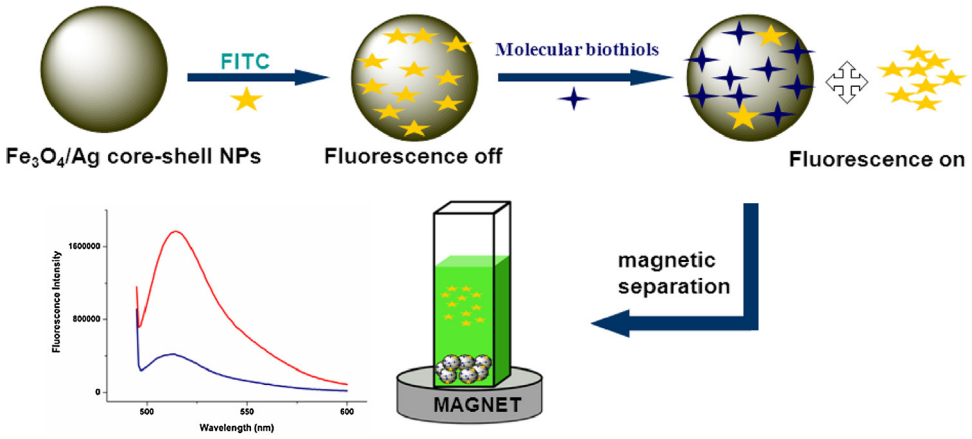

Fig. 1. Schematic representation of the mechanism of biothiols sensing system based on FITC modified magnetic core–shell Fe_3O_4/Ag hybrid nanoparticles.

average size was estimated to be 217 nm, which was allowed to be overestimated comparing with that of SEM images. The magnetic property was also evidenced by magnet test as the inset photographic image shown (Fig. S2A), the absorbance peak disappeared after the magnetic separation as indicated by curve b.

3.2. Sensing mechanism

Fig. 1 outlines the assumed response mechanism of the sensor for biothiols. Firstly, the surface of prepared magnetic Fe_3O_4/Ag hybrid nanoparticles was modified by FITC molecules through S═C═N— groups with non-covalent adsorption by Ag–SCN linkage and the fluorescence of FITC was quenched. It has been reported that, silver nanoparticles exhibit high FRET (fluorescence resonance energy transfer)-related quenching efficiency to organic fluorophores [32]. Herein, silver shell acted as the carrier and fluorescence quencher of FITC. Upon the addition of biothiols, the FITC molecules were effectively exchanged by thiol groups and released from the surface of the silver shell, which can be attributed to the stronger affinity between thiol groups and silver surface. Away from the quencher, the fluorescence of FITC recovered. The fluorescence signal for exchange was reflected by the photoemission of FITC in the solution. FITC was properly employed as a fluorescence reporter in the present study. To avoid the disturbance of un-stabilizing conditions, the clear solution was separated from hybrid particles by magnetic fields and then was measured by fluorescence spectrometer. The magnetic Fe_3O_4 core-nanoparticles provided a simple and rapid separation process and worked well. As the fluorescence spectra shown in Fig. 1, the fluorescence intensity of the solution increased after incubating with molecular biothiols (red curve) compared with that of the absence of thiol molecules (navy curve), indicating the fact that the FITC molecules on the surface of silver hybrid nanoparticles were effectively exchanged by biothiol molecules.

Interestingly, the place-displacement between FITC and biothiol molecules could be confirmed by the theory of hard and soft acids and bases (HSAB). Ag^+ ions, as the soft acids, were prone to conjunct with much softer bases, so the stronger interaction tendency exhibited between silver atoms and thiol groups comparing with S═C═N— groups. Thus, the SCN-containing FITC molecule was able to be replaced by biothiol molecules and released from the surface of silver shell. Besides, it was also noteworthy that the energy of Ag—S bond was larger than that of Ag–SCN [33], which suggested the stronger interaction tendency between the silver surface atoms and the thiol groups, and thus, the FITC molecules could be substituted by biothiol molecules. Therefore, a sensing system for chromogenic detection of biothiols was presented based on fluorescence recovery of FITC.

Furthermore, the displacement of FITC was verified by infrared spectroscopy. As displayed in Fig. S3, after the incubation with GSH, the typical peak at 1570 cm^{-1} (C═S) disappeared, and the peak at 1640 cm^{-1} (N—H) increased. The results clearly demonstrated that the FITC was replaced by GSH on the surface of Fe_3O_4/Ag nanoparticles.

3.3. Optimization of sensing conditions

As a typical biological thiol, GSH was used to further investigate the fluorescence response of the sensing system. The effects of pH, temperature and incubation time were studied to optimize the experimental protocol. The fluorescence intensity with emission at 514 nm was acquired and the value of $(F_{GSH} - F_{blank})/F_{blank}$ was employed for the estimation experiments, where F_{GSH} means the fluorescence intensity at 514 nm of clear solution after the nanoparticles have been incubated for a given time interval at the desired temperature followed by the addition of GSH, F_{blank} means that without the addition of GSH.

Interestingly, the replacement of FITC by biothiol molecules was found pH related. Figure S4 displays fluorescence responses to different pH values of the sensing system in presence of GSH. As the results indicated, there was an optimum pH value for GSH response, and pH at 5.8 was selected for GSH in the following experiments, which was equal or close to its isoelectric point.

The incubation temperature and time might play important roles in the sensing sensitivity. Several important experiments were performed to test their effects. Initially, fluorescence intensity of the nanoparticles equilibrated with the buffer as a function of time at various temperatures was determined and displayed, as shown in Fig. S5A. The results suggested that the fluorescence intensity of the nanoparticles equilibrated with buffer slightly increased as function of time and temperature, but that did not match the increase caused by thiols according to the following results with GSH.

The FITC modified nanoparticles and GSH were equilibrated at different temperatures, and the fluorescence recovery was acquired with emission at 514 nm. $(F_{GSH} - F_{blank})/F_{blank}$ was employed as the index, which could deduct possible systematic errors. Herein, F_{GSH} means the fluorescence intensity at 514 nm of clear solution after the nanoparticles have been incubated for a given time interval at the desired temperature followed by the addition of 10 μM GSH, F_{blank} means that without the addition of GSH. As shown in Fig. S5B, the fluorescence signal of the solution increased gradually with the

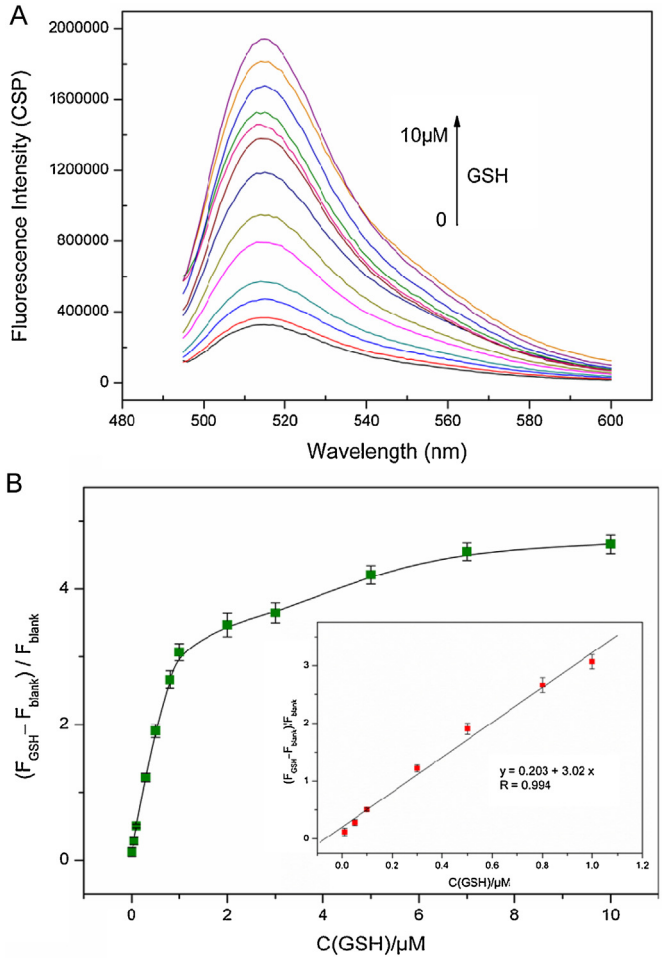

Fig. 2. (A) Fluorescence responses of the clear solution after the addition of different concentrations of GSH in the mixture of nanoparticles and sodium acetate buffer solution. (B) A plot of $(F_{GSH} - F_{blank})/F_{blank}$ versus the different concentrations of GSH. Inset shows a linear relationship in the range from 10 nM to 1000 nM. The error bars represent standard deviations based on three independent measurements.

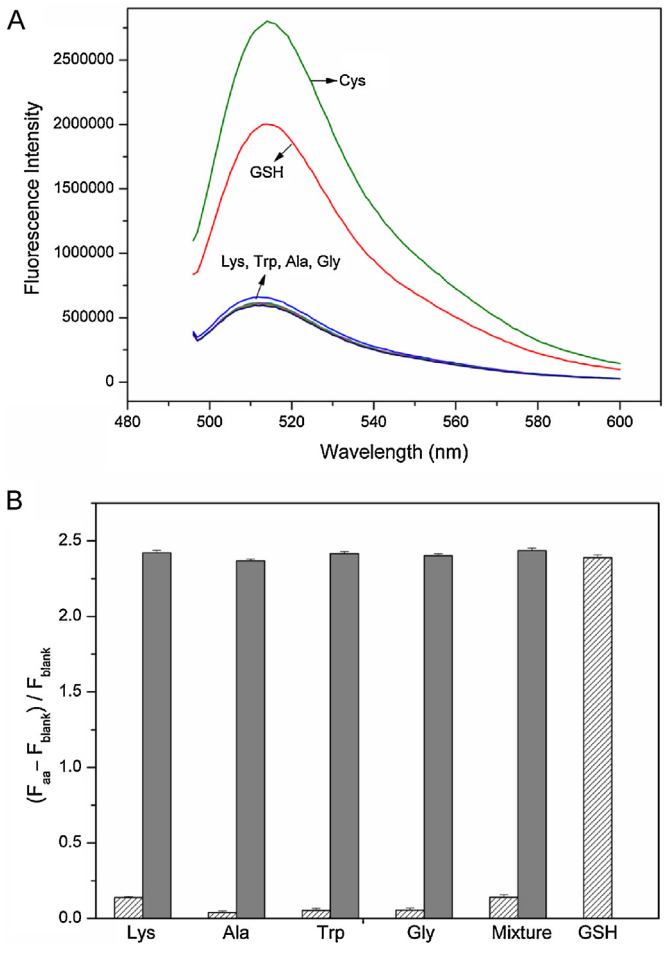

Fig. 3. (A) Fluorescence spectra of this assay in the presence of GSH and Cys (1.0 μM) and other amino acids (Lys, Ala, Trp, Gly) under the concentration of 10 μM, respectively. (B) Fluorescence response of the sensing system to 1.0 μM of GSH or 10 μM of other amino acids (the dense bar portion) and to the mixture of 10 μM of other amino acids with 1.0 μM of GSH (the gray bar portion). Error bars are standard deviations across three repetitive experiments.

increasing of temperature. Considering the application in physiological conditions, 37 °C was selected. Moreover, 20 min was chosen for incubation in the following assays.

3.4. Determination of sensitivity and selectivity for biothiols

Under the above optimized conditions, the determination performance of typical biothiols by using this sensing method was investigated. Different concentrations of biothiols were added to the nanoparticle solution and incubated for 20 min at 37 °C. After magnetic separation, the fluorescence spectra of clear solutions were recorded (λ_{ex} = 490 nm). Fig. 2A shows the fluorescence response of the sensing method against different concentrations of GSH. The fluorescence intensity ratio value of $(F_{GSH} - F_{blank})/F_{blank}$ was employed for the quantification of GSH, where F_{blank} means the fluorescence intensity of clear solution separated from nanoparticles without GSH after incubated for 20 min as the ones with GSH. It can be seen that the $(F_{GSH} - F_{blank})/F_{blank}$ increased with the increasing concentrations of GSH. A typical plot of the $(F_{GSH} - F_{blank})/F_{blank}$ values versus GSH concentrations was shown in Fig. 2B and a good linear relationship was exhibited over the range of 10–1000 nM, with relative standard deviations (RSD) between 4.3% and 12.0%. Moreover, another aminothiol, Cys, was also tested for this method. Similarly, under the optimum pH value at 5.0 (seen in Fig. S6), the satisfying results for Cys molecules were obtained, that is, as observed in Fig. S7, a good linear relationship of $(F_{Cys} - F_{blank})/F_{blank}$ values against Cys concentrations was displayed in the range from 20 to 1000 nM with RSD between 0.8% and 10.8%. The limits of detection for GSH and Cys were attained of 10 nM and 20 nM, respectively, lower than common colorimetric methods [22,24,27]. These results demonstrated the fluorescence off-on sensing strategy based on place-substitution could highly sensitively and highly accurately quantify the biothiols.

Meanwhile, the coverage and displacement of FITC are required to investigate for verifying the sensing accuracy and authenticity. According to the Lambert–Beer law, and the correlation between fluorescence intensity I_F and concentration C,

$$A = -\log T = -\log \frac{I_t}{I_0} = K\varepsilon(\lambda)bC \quad (1)$$

$$I_F = 2.303 I_0 Y_F \varepsilon(\lambda) bC \quad (2)$$

In Eq. (1), A means absorbance, I_0 and I_t mean the intensity of incident light and transmission light, K means the related coefficient, $\varepsilon(\lambda)$ is molar absorption coefficient, b represents the layer thickness, C means the concentration of analyte. In Eq. (2), I_F means the fluorescence intensity, Y_F means the fluorescence quantum yield.

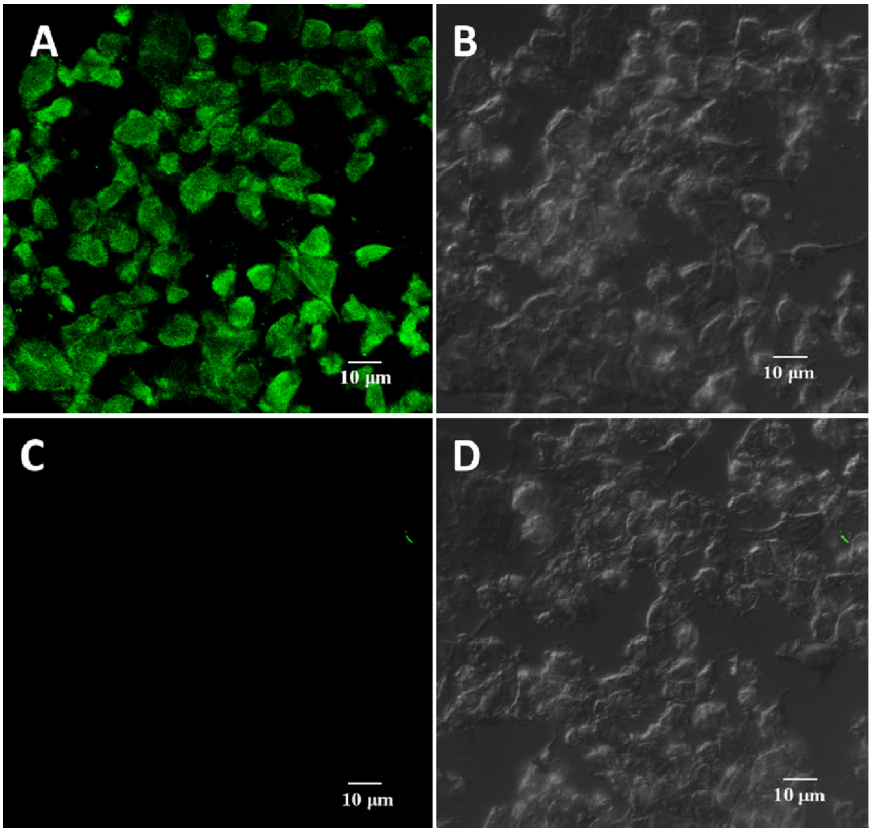

Fig. 4. Confocal fluorescence images in Hela cells that were treated with the FITC modified Fe_3O_4/Ag hybrid nanoparticles. (A) Cells stained with nanoparticles, (B) bright field image of cells shown in (A), (C) cells treated with NEM and then incubated with nanoparticles, and (D) bright field image of cells shown in (C). Scale bar is 10 μm.

For a certain kind of analyte, an equality $I_F(1)$ could be obtained from Eq. (1) and (2),

$$\frac{I_F(1)}{C(1)} = \frac{I_F(2)}{C(2)} \quad (3)$$

where $I_F(1)$ is the intensity of FITC at the concentration of 10^{-6} mol/L, $C(1)$ means a known concentration of 10^{-6} mol/L, $I_F(2)$ is the intensity of the clear solution separated from nanoparticles after 30 min incubation with GSH at 40 °C, expecting complete displacement of FITC. Thus the concentration of FITC in clear solution of each sensing system could be obtained by the equality $C(2) = I_F(2)C(1)/I_F(1)$. According to the fluorescence intensity recorded in Table S1, the concentration of FITC in each sensing system was estimated to be 0.89 μM, which means higher than 0.89 μM of the given thiols are required in order to completely displace the FITC molecules from the nanoparticle surface. This result was included in the linear range from 10 nM to 1 μM, and therefore the quantitation for biothiols was rationally feasible.

To validate the sensing selectivity toward biothiols, some other amino acids such as Lys, Ala, Trp and Gly were employed for the further test. Initially, these analytes were tested in the sensing solution separately. As shown in Fig. 3A, it is clear to see that only thiol-containing analytes, GSH and Cys, can induce the obvious recovery of fluorescence of FITC due to the higher affinity of Ag—S than Ag–SCN. Moreover, it is worth taking consideration that the Cys induced recovery of fluorescence of FITC was stronger than that of GSH in presence of the same concentration. Molecular space steric hindrance could be employed to explain the different place-displacement ability for the FITC molecules. The Cys molecules were more easily to attach to the surface of modified nanoparticles with weaker space steric hindrance due to smaller molecular weight. The specificity toward a series of thiols has been reported based on gold nanoparticles or organic dyes [28,34]. To further highlight the specificity and selectivity toward thiols, the fluorescence response to the GSH at 1.0 μM in the presence of other amino acids respectively, and the mixture of GSH and all of other amino acids, were all investigated. As indicated in Fig. 3B, no noticeable interference in the detection system was observed on addition of other amino acids. It indicated that the developed sensing system could highly selectively determine molecular biothiols.

3.5. Application of this sensor in living cell imaging

After establishing the sensing system for highly sensitive and highly selective determination of biothiols, we next assessed whether it could respond in real bio-systems. Hela cells were taken as the biological test models owing to their strong phagocytic activity and clinical significance. This sensing system was utilized to image intracellular GSH which was the most abundant thiol species in cells and involved in many important biochemical processes. Hela cells placed on coverslips were washed with PBS, followed by incubating with 1 mg/mL of the FITC modified hybrid nanoparticles at 37 °C for 30 min, allowing the uptake of nanoparticles, and then washed with PBS three times. A strong fluorescence signal was observed from the Hela cells, as shown in Fig. 4A. In the control experiment, Hela cells were pretreated with an excess of thiol-reactive NEM [35] which consumed all of the free thiols within the cells, and then incubated with the sensing nanoparticles after washing three times with PBS. There was hardly any fluorescence, as observed in Fig. 4C. Fig. 4B and D provided the bright field images corresponding to Fig. 4A and C, respectively. So the sensing system could be established to be practically applicable, and the fluorescence changes in living cells indeed result from the changes of intracellular thiol levels. These results demonstrated that the

place-displacement between biothiol molecules and FITC could occur in living cells and indicated that our presented strategy was capable of sensing thiols in real biological systems.

4. Conclusions

In summary, we have designed a chromogenic strategy for selective determination of molecular biothiols and fluorescent imaging in living cells by using FITC modified magnetic core–shell Fe_3O_4/Ag nanoparticles, due to the stronger interaction between silver surface and thiol groups. This assay method exhibits excellent selectivity and sensitivity toward typical biothiols such as GSH and Cys. Importantly, our sensing system did not involve the water solubility and aggregation problems comparing with other methods. Furthermore, the present sensor had been successfully employed for the fluorescent imaging of intracellular GSH in living cells, which might hold a promising potential for application in biological systems.

Acknowledgements

This work was financially supported by the Scientific Research Foundation for the Returned Overseas Chinese Scholars, State Education Ministry, the Innovation Projects of the Chinese Academy of Sciences (Grant KZCX2-EW-206), the National Research Foundation of Korea (Grant R11-2008-0061852 and K20904000004-12A0500-00410), the Program of Zhejiang Provincial Natural Science Foundation of China (Grant R5110230) and the 100 Talents Program of the Chinese Academy of Sciences.

Appendix A. Supplementary data

Supplementary data associated with this article can be found, in the online version, at http://dx.doi.org/10.1016/j.snb.2013.12.053.

References

[1] V. Miller, D. Lawrence, T. Mondal, R. Seegal, Reduced glutathione is highly expressed in white matter and neurons in the unperturbed mouse brain — implications for oxidative stress associated with neurodegeneration, Brain Res. 1276 (2009) 22–30.
[2] S. Seshadri, A. Beiser, J. Selhub, P. Jacques, I. Rosenberg, R. D'Agostino, P. Wilson, P. Wolf, Plasma homocysteine as a risk factor for dementia and Alzheimer's disease, N. Engl. J. Med. 346 (2002) 476–483.
[3] J. Matés, C. Pérez-Gómez, M. Blanca, Chemical and biological activity of free radical 'scavengers' in allergic diseases, Clin. Chim. Acta 296 (2000) 1–15.
[4] S. Opalenik, Q. Ding, S. Mallery, J. Thompson, Glutathione depletion associated with the HIV-1 TAT protein mediates the extracellular appearance of acidic fibroblast growth factor, Arch. Biochem. Biophys. 351 (1998) 17–26.
[5] J. Sung, S. Shin, H. Park, R. Montelaro, Y. Chong, Protective effect of glutathione in HIV-1 lytic peptide 1-induced cell death in human neuronal cells, J. Neurovirol. 7 (2001) 454–465.
[6] G. Bijur, R. Davis, R. Jope, Rapid activation of heat shock factor-1 DNA binding by H_2O_2 and modulation by glutathione in human neuroblastoma and Alzheimer's disease cybrid cells, Mol. Brain Res. 71 (1999) 69–77.
[7] G. Pagano, A. Zatterale, P. Degan, M. D'Ischia, F.J. Kelly, F.V. Pallardo, R. Calzone, G. Castello, C. Dunster, A. Giudice, Y. Kilinc, A. Lloret, P. Manini, R. Masella, E. Vuttariello, M. Warnau, In vivo prooxidant state in Werner syndrome (WS): results from three WS patients and two WS heterozygotes, Free Radical Res. 39 (2005) 529–533.
[8] Z. Wood, E. Schroder, J. Harris, L. Poole, Structure, mechanism and regulation of peroxiredoxins, Trends Biochem. Sci. 28 (2003) 32–40.
[9] S. Shahrokhian, Lead phthalocyanine as a selective carrier for preparation of a cysteine-selective electrode, Anal. Chem. 73 (2001) 5972–5978.
[10] A. Ivanov, I. Nazimov, L. Baratova, Qualitative and quantitative determination of biologically active low-molecular-mass thiols in human blood by reversed-phase high-performance liquid chromatography with photometry and fluorescence detection, J. Chromatogr. A 870 (2000) 433–442.
[11] G. Chwatko, E. Bald, Determination of cysteine in human plasma by high-performance liquid chromatography and ultraviolet detection after pre-column derivatization with 2-chloro-1-methylpyridinium iodide, Talanta 52 (2000) 509–515.
[12] G. Chen, L. Zhang, J. Wang, Miniaturized capillary electrophoresis system with a carbon nanotube microelectrode for rapid separation and detection of thiols, Talanta 64 (2004) 1018–1023.
[13] T. Inoue, J. Kirchhoff, Determination of thiols by capillary electrophoresis with amperometric detection at a coenzyme pyrroloquinoline quinone modified electrode, Anal. Chem. 74 (2002) 1349–1354.
[14] M. MacCoss, N. Fukagawa, D. Matthews, Measurement of homocysteine concentrations and stable isotope tracer enrichments in human plasma, Anal. Chem. 71 (1999) 4527–4533.
[15] L. Nie, H. Ma, M. Sun, X. Li, M. Su, S. Liang, Direct chemiluminescence determination of cysteine in human serum using quinine-Ce(IV) system, Talanta 59 (2003) 959–964.
[16] C. Lau, X. Qin, J. Liang, J. Lu, Determination of cysteine in a pharmaceutical formulation by flow-injection analysis with a chemiluminescence detector, Anal. Chim. Acta 514 (2004) 45–49.
[17] T. Inoue, J. Kirchhoff, Electrochemical detection of thiols with a coenzyme pyrroloquinoline quinone modified electrode, Anal. Chem. 72 (2000) 5755–5760.
[18] W. Wang, L. Li, S. Liu, C. Ma, S. Zhang, Determination of physiological thiols by electrochemical detection with piazselenole and its application in rat breast cancer cells 4T-1, J. Am. Chem. Soc. 130 (2008) 10846–10847.
[19] M. Zhang, M. Yu, F. Li, M. Zhu, M. Li, Y. Gao, L. Li, Z. Liu, J. Zhang, T. Yi, C. Huang, A highly selective fluorescence turn-on sensor for cysteine/homocysteine and its application in bioimaging, J. Am. Chem. Soc. 129 (2007) 10322–10323.
[20] C. Lim, G. Masanta, H. Kim, J. Han, H. Kim, B. Cho, Ratiometric detection of mitochondrial thiols with a two-photon fluorescent probe, J. Am. Chem. Soc. 133 (2011) 11132–11135.
[21] L. Niu, Y. Guan, Y. Chen, L. Wu, C. Tung, Q. Yang, BODIPY-based ratiometric fluorescent sensor for highly selective detection of glutathione over cysteine and homocysteine, J. Am. Chem. Soc. 134 (2012) 18928–18931.
[22] F. Zhang, L. Han, L. Israel, J. Daras, M. Maye, N. Ly, C. Zhong, Colorimetric detection of thiol-containing amino acids using gold nanoparticles, Analyst 127 (2002) 462–465.
[23] S. Durocher, A. Rezaee, C. Hamm, C. Rangan, S. Mittler, B. Mutus, Disulfide-linked, gold nanoparticle based reagent for detecting small molecular weight thiols, J. Am. Chem. Soc. 131 (2009) 2475–2477.
[24] N. Uehara, K. Ookubo, T. Shimizu, Colorimetric assay of glutathione based on the spontaneous disassembly of aggregated gold nanocomposites conjugated with water-soluble polymer, Langmuir 26 (2010) 6818–6825.
[25] Q. Xiao, F. Shang, X. Xu, Q. Li, C. Lu, Specific detection of cysteine and homocysteine in biological fluids by tuning the pH values of fluorosurfactant-stabilized gold colloidal solution, Biosens. Bioelectron. 30 (2011) 211–215.
[26] C. Wu, Q. Xu, Stable and functionable mesoporous silica-coated gold nanorods as sensitive localized surface plasmon resonance (LSPR) nanosensors, Langmuir 25 (2009) 9441–9446.
[27] C. Li, C. Wu, J. Zheng, J. Lai, C. Zhang, Y. Zhao, LSPR sensing of molecular biothiols based on noncoupled gold nanorods, Langmuir 26 (2010) 9130–9135.
[28] R. Wang, L. Chen, P. Liu, Q. Zhang, Y. Wang, Sensitive near-infrared fluorescent probes for thiols based on SeN bond cleavage: imaging in living cells and tissues, Chem. Eur. J. 18 (2012) 11343–11349.
[29] R. Wang, F. Yu, L. Chen, H. Chen, L. Wang, W. Zhang, A highly selective turn-on near-infrared fluorescent probe for hydrogen sulfide detection and imaging in living cells, Chem. Commun. 48 (2012) 11757–11759.
[30] H. Deng, X. Li, Q. Peng, X. Wang, J. Chen, Y. Li, Monodisperse magnetic single-crystal ferrite microspheres, Angew. Chem. Int. Ed. 44 (2005) 2782–2785.
[31] Q. Zhang, L. Yang, J. Zhang, J. Guan, Y. Wang, Preparation of magnetic core–shell Fe_3O_4/Ag nanoparticles and its properties, J. Chin. Ceram. Soc. 35 (2007) 987–990.
[32] H. Nabika, S. Deki, Enhancing and quenching functions of silver nanoparticles on the luminescent properties of europium complex in the solution phase, J. Phys. Chem. B 107 (2003) 9161–9164.
[33] D. Hatchett, R. Uibel, K. Stevenson, J. Harris, H. White, Electrochemical measurement of the free energy of adsorption of n-alkanethiolates at Ag(1 1 1), J. Am. Chem. Soc. 120 (1998) 1062–1069.
[34] O. Rusin, N. Luce, R. Agbaria, J. Escobedo, S. Jiang, I. Warner, F. Dawan, K. Lian, R. Strongin, Visual detection of cysteine and homocysteine, J. Am. Chem. Soc. 126 (2004) 438–439.
[35] W. Henne, D. Doorneweerd, A. Hilgenbrink, S. Kularatne, P. Low, Synthesis and activity of a folate peptide camptothecin prodrug, Bioorg. Med. Chem. Lett. 16 (2006) 5350–5355.

Biographies

Ling Chen received her BS degree in chemistry in 2009 from Shandong University, China and joined the Laboratory of Environmental Microanalysis and Monitoring in Yantai Institute of Coastal Zone Research, Chinese Academy of Sciences. She is studying for her PhD degree. Her current research interest is optical sensors for environmental analysis using novel nanomaterials.

Jinhua Li received her PhD in analytical chemistry from the Department of Chemistry of Hong Kong Baptist University, Hong Kong SAR, China, in 2009. In the same year, she joined the Laboratory of Environmental Microanalysis and Monitoring in Yantai Institute of Coastal Zone Research, Chinese Academy of Sciences, as an assistant professor. Her current research interest focuses on preparation of novel molecular imprinting polymers and applications to sample pretreatment and bio/chemosensors.

Shasha Wang received her BS degree in chemistry from Qufu Normal University, China in 2010. During the same year, she joined the Laboratory of Environmental Microanalysis and Monitoring in Yantai Institute of Coastal Zone Research, Chinese Academy of Sciences. Her current research interests focus on investigation of novel nanomaterials for understanding of nanotoxicity and application as optical sensors for environmental analysis.

Wenhui Lu received her MS degree in environmental science in 2010 from Qingdao Technological University and joined the Laboratory of Environmental Microanalysis and Monitoring in Yantai Institute of Coastal Zone Research, Chinese Academy of Sciences. Her current research interest is chromatographic separation techniques.

Aiguo Wu is a professor and postgraduate tutor in Ningbo Institute of Materials Technology and Engineering, Chinese Academy of Sciences from 2009 and engages in the applications of various nanomaterials in biomedicine, bioanalytical chemistry/environmental sciences and nanostructures fabricated based on biomacromolecules study.

Jaebum Choo is a Professor in the Department of Bionano Engineering at Hanyang University. He is a Director of Integrated Human Sensing System Research Center (ERC). He is also a Vice-Director of Hanyang Biomedical Research Institute now. He received his Ph.D. from Texas A&M University in 1994. He has published more than 160 papers in peer-reviewed SCI journals and has given over 90 invited lectures till now. His research interest is mainly centered on (a) development of integrated human sensing system for early diagnosis of intractable diseases, (b) SERS-based molecular imaging of specific biomarker expressed on cancer cells, and (c) development of fast and sensitive immunoassay technique using optofluidic nanosensor.

Lingxin Chen received his PhD in analytical chemistry from Dalian Institute of Chemical Physics, Chinese Academy of Sciences, China, in 2003. After two years postdoctoral experience in the Department of Chemistry, Tsinghua University, China, he joined first as a BK21 researcher and then as a research professor in the Department of Applied Chemistry, Hanyang University, Ansan, Korea, in 2006. Now he is a professor in Yantai Institute of Coastal Zone Research, Chinese Academy of Sciences. His current research interests include chromatographic separation techniques and optical sensor technologies for environmental analysis using novel properties of materials such as functionalized nanoparticles and molecularly imprinted polymers.